ELSEVIER

Journal of Molecular Structure 565–566 (2001) 59–67

Journal of
MOLECULAR
STRUCTURE

www.elsevier.nl/locate/molstruc

Spectroscopic characterization of α- and γ-pyrones and their substituted 4-hydroxy and 4-methoxy derivatives: an integrated infrared, photophysical and theoretical study

J. Seixas de Melo*, G. Quinteiro, J. Pina, S. Breda, R. Fausto

Department of Chemistry (CQC), University of Coimbra, 3004-535 Coimbra, Portugal

Received 31 August 2000; revised 14 November 2000; accepted 14 November 2000

Abstract

The simple α- and γ-pyrones and the substituted 6-methyl, 4-hydroxy and 4-methoxy α-pyrones were investigated in relation to their spectroscopic properties. The characterization involves vibrational and electronic spectroscopy. IR spectra for the ground electronic state of the studied compounds at room temperature were obtained and interpreted taking into consideration the simulated ab initio (6-31G*) data. The most important canonical structures accounting for the properties of the ground state were determined for each compound and several photophysical properties were evaluated: electronic spectra, oscillator strengths and the emission properties (both fluorescence and phosphorescence) in media of different polarity. The origin of the first singlet and triplet excited states is also discussed. In addition, the energies of the electronic transitions were estimated using semi-empirical molecular orbital calculations, the calculated results showing an excellent agreement with the experimental data.

Keywords: Pyrones; Electronic structure; Photophysics; Vibrational spectra; Molecular orbital calculations

1. Introduction

Alpha and gamma pyrones are the fundamental moieties of several naturally occurring compounds and synthetic pesticides. In the first case, several compounds, such as the coumarins, psoralens and chromones, are known to be potent photosensitizers [1]. In the second case, several pesticides of rodenticidal activity belonging to the coumarin family, such as Warfarin©, Coumaphos© and Potasan©, possess the α-pyrone nucleus present in its fundamental core [2,3]. Additionally, these pyrones are very useful synthetic reagents as in the Diels–Alder reaction. Despite the large number of publications related to the more complex photosensitizers mentioned above, there is little spectroscopic and photophysical knowledge of the simple and fundamental α- and γ-pyrones. The assignment of the state order and their consequence on the photophysics and photochemistry of α- and γ-pyrones is of great interest since it will allow the understanding of the more complex coumarin and chromone derivatives. In this study, two substituted α-pyrones, with hydroxyl and methoxy groups were also considered (4-hydroxy-6-methyl-α-pyrone, 4HMP, and 4-methoxy-6-methyl-α-pyrone, 4MMP). For these compounds, in the triplet state a peculiar behavior was observed.

* Corresponding author. Tel.: +351-39-852-080; fax: +351-39-827-703.

E-mail addresses: sseixas@ci.uc.pt (J. Seixas de Melo), rfausto@ci.uc.pt (R. Fausto).

0022-2860/01/$ - see front matter
PII: S0022-2860(00)00944-3

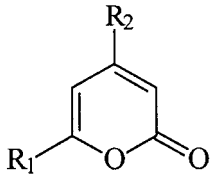

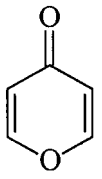

R_1=R_2= H	α-pyrone	γ-pyrone
R_1=CH_3 R_2= OH	4HMP	
R_1=CH_3 R_2= OCH_3	4MMP	

We shall show in this article that careful interpretation of the absorption spectra (including determination of oscillator strengths), fluorescence quantum yields and phosphorescence lifetimes as a function of solvent polarity, enables us to conclude that the lowest singlet excited state is of n,π* character, whereas the lowest triplet excited states are π,π*. Semi-empirical INDO/S and ZINDO/S calculations with extensive configuration interaction (CI — up to 201 singly excited configurations) also support these assignments.

2. Experimental

All compounds use were commercially obtained (Alldrich). Solvents were of spectroscopic grade and purified by standard methods before use.

Absorption spectra were obtained in solution (1×10^{-5} to 10^{-6} M) using a Shimadzu UV-2100 or Olis-Cary14 converted spectrometer. Fluorescence and phosphorescence experiments were undertaken in a Jobin-Ivon SPEX Fluorog 3-22 spectrometer (the latter using the D1934 unit), all spectra being corrected for the wavelength response of the system. The fluorescence quantum yields were measured using several standards namely: 2,2′-bithiophene ($\phi_F = 0.014$ in ethanol [4]) and 3-chloro-7-methoxy-4-methylcoumarin ($\phi_F = 0.12$ in cyclohexane [5]). Phosphorescence quantum yields were measured by comparison with benzophenone, $\phi_P =$ 0.85 [6]. Oscillator strengths were obtained from the experimental integrated intensities, according to the equation: $f = 4.315 \times 10^{-9} \int \varepsilon(\bar{\nu})\, d\bar{\nu}$.

Infrared studies were performed on the pure compounds using an FTIR Mattson Infinity Series spectrometer, equipped with a germanium/KBr beam splitter and a deuterated triglycine sulphide (DTGS) detector fitted with KBr windows.

The ab initio molecular orbital calculations were performed using the 6-31G* basis set [7] with the GAUSSIAN 94 program package [8] running on a DEC ALPHA 7000 computer. The normal coordinate calculations were made using the ab initio force constants with the programs BUILD-G, TRANSFORMER and VIBRAT [9,10]. A single scaling factor (0.89) was applied to the calculated frequencies. The semi-empirical calculations were performed with the AM1, ZINDO/S and INDO1/S Hamiltonians [11–13] using MOPAC (version 6.0) [14], HYPERCHEM (release 3, for Windows) [15] and ARGUS™ (version 1.2) [16], respectively. Up to 201 singly or singly and doubly excited configurations were used in the semi-empirical CI calculations.

3. Results

Figs. 1–4 show: (1A) the absorption spectra of α- and γ-pyrone in cyclohexane and ethanol, (1B) the absorption spectra of γ-pyrone in dioxane/water mixtures; (2) the fluorescence spectra of α-pyrone and 4HMP in methylcyclohexane and 4MMP in ethanol; (3) the phosphorescence spectra of 4HMP and 4MMP in different solvents; and (4) the triplet–triplet absorption spectra of the four pyrones in dioxane. Table 1 compares experimental absorption maxima and oscillator strengths with the corresponding semi-empirical ZINDO/S-CI, INDO/1-CI and AM1-CI calculated values. Table 2 provides data on the: (1) fluorescence and phosphorescence maxima; (2) fluorescence quantum yields; (3) phosphorescence lifetimes; and (4) $T_1 \rightarrow T_n$ absorption maxima and triplet lifetimes, for all the pyrones studied. Table 3 provides ab initio calculated selected bond lengths and bond stretching frequencies and the corresponding observed IR frequencies. Fig. 5 shows the calculated ab initio 6-31G* Mülliken atomic charges in α- and γ-pyrone.

4. Discussion

Important points in the following discussion are: (i) the assignment of the lowest singlet and triplet states to n,π* or π,π* states; (ii) the type of

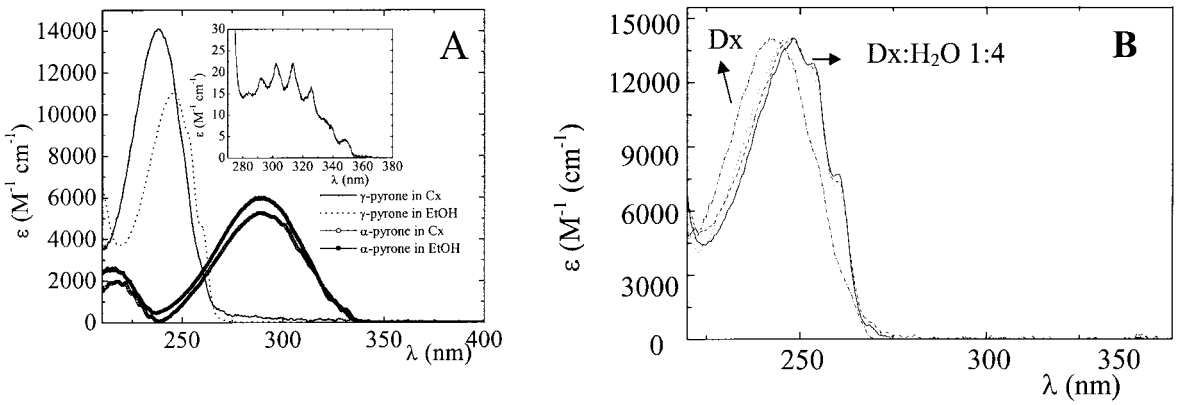

Fig. 1. (A) Absorption spectra of α- and γ-pyrone in cyclohexane and ethanol, and (B) absorption spectra of γ-pyrone in dioxane/water mixtures. Inserted in (A) is the magnified region between 270 and 380 nm, for g-pyrone in cyclohexane.

molecular species existing in the ground-state and first singlet and triplet excited states; and (iii) the characterization of the electron distribution in the ground state. The results obtained for the different molecules studied, in particular the two simplest pyrones, will be systematically compared in order to evaluate the effect of changing the position of the oxygen atom in the pyrone ring on the molecular properties.

4.1. Singlet state properties

Our first consideration will be the assignment of the state order for the two lowest singlet excited states. We shall focus on absorption data, their solvent dependence and fluorescence quantum yields.

In nonpolar solvents, such as cyclohexane, the absorption spectra of γ-pyrone exhibit two well-separated bands: an intense band, with maximum at 238 nm, and a much less intense band, vibrationally resolved, with maximum at ca. 302 nm (Fig. 1A). The extinction coefficients of these bands are consistent with a state of π,π^* origin as being responsible for the lower wavelength transition and a state of n,π^* origin for the longer one. Indeed, it is well known that when the less intense n,π^* band can be observed, the assignment of both π,π^* and n,π^* bands is straightforward, as in the classical example of benzophenone [6]. Moreover, theoretical data support the assignments made (see Table 1). Our general experience in comparing calculated and observable $n \rightarrow \pi^*$ transitions indicates that if the theory predicts an n,π^* state approximately $\geq 2000\ cm^{-1}$ below a π,π^* state, then it is likely that the predicted ordering is correct [17].

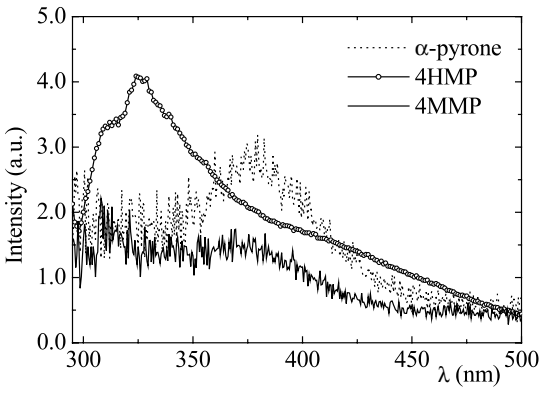

Fig. 2. Fluorescence spectra of α-pyrone and 4HMP in methylcyclohexane and 4MMP in ethanol.

In polar solvents, such as ethanol, the most intense band is red shifted and the less intense is blue shifted, so that they overlap partially. In Fig. 1A, the presence of the n,π^* feature underneath the most intense π,π^* band can be clearly noticed, leading to the observed increase in vibrational resolution of the long wavelength shoulder of the band. Moreover, absorption studies undertaken for γ-pyrone in dioxane/water mixtures with increasing water content show that both the observed gradual red shift of the π,π^* band and the increase of the vibrational resolution of its

Table 1
Experimental and theoretical data for the first two lowest transition energy ($S_{1,2} \leftarrow S_0$) and oscillator strength, f, for the pyrones studied. The experimental oscillator strengths were obtained as described in Section 2

Compound	Transition	Experimental			ZINDO/S-CI		AM1-CI	INDO/S-CI	
		λ_{abs}^{max} (*nm*)	ε (M^{-1} cm^{-1})	f	λ (nm)	f	λ (nm)	λ (nm)	f
γ-pyrone	$S_1 \leftarrow S_0$	302 348 (0–0)	200	0.0005	389	($\leq 10^{-4}$)	264	413	($\leq 10^{-5}$)
	$S_2 \leftarrow S_0$	238	14100	0.394	236	0.491	251	249.5	0.4888
α-pyrone	$S_1 \leftarrow S_0$	331,325	560,980	0.005	323	0.0005	306	340	0.0005
	$S_2 \leftarrow S_0$	286	5353	0.15	284	0.31	260	310	0.2699
4HMP	$S_1 \leftarrow S_0$	330 (onset)	≈ 100	[a]	310	0.0006n,π^*	322	331	0.0006
	$S_2 \leftarrow S_0$	287	5980	0.15	293	0.30π,π^*	258	303	0.3358
4MMP	$S_1 \leftarrow S_0$	325 (onset)	≈ 100	[a]	309	0.0007n,π^*	315	331	0.0006
	$S_2 \leftarrow S_0$	281	5815	0.10	285	0.31π,π^*	253	298	0.3304

[a] Not determined because no clear band could be observed due to overlap of S_2 (π,π^*).

long wavelength shoulder (due to more extensive partial overlap with the n,π^* band) correlate well with the increase of the polarity of the media. So, although the state order does not change, the two lowest excited states are considerably closer in energy in polar than in non-polar media.

In the case of α-pyrone, the absorption spectrum in cyclohexane looks similar to those of γ-pyrone in polar solvents. In particular, it presents significant vibrational resolution in the long wavelength shoulder of the band ascribable to the π,π^* transition (Fig. 1B), which, as described above, can be attributed to an overlap with the n,π^* band. In more polar solvents (e.g. ethanol, see Fig. 1B) the $\pi-\pi^*$ band is slightly red shifted and the vibrational resolution disappears because

Table 2
Absorption and photophysical properties of the pyrones in different solvents. Fluorescence and phosphorescence wavelength maxima (λ_{em} ($S_1 \rightarrow S_0$), λ_{em} ($T_1 \rightarrow S_0$)) and quantum yields (ϕ_F, ϕ_P), phosphorescence lifetimes (τ_{Ph}), triplet–triplet absorption maximum ($T_1 \rightarrow T_n$) and triplet lifetimes (τ_T)

Compound	Solvent	λ_{em} ($S_1 \rightarrow S_0$) (nm)	λ_{em} ($T_1 \rightarrow S_0$) (nm)	ϕ_F	ϕ_P	τ_{Ph} (s)	$T_1 \rightarrow T_n$[a] maxima (nm)	τ_T (μs)[a]
α-pyrone	MCH			2.6×10^{-4}	–	–	300	1.8
	Ethanol	380	492		8.4×10^{-4}	0.62		
	Ethanol:HCl	–	499		8.4×10^{-4}	0.49		
γ-pyrone	MCH	[b]		[b]	–		370	14
	Ethanol		437		0.05	0.90		
	Ethanol:HCl		437	–		0.94		
4HMP	MCH	326			–		320,360	3.5
	Ethanol	326,380	464	5.5×10^{-4}	4×10^{-3}	0.48		
	Ethanol:HCl	–	458		8×10^{-3}	0.55		
4MMP	MCH	326	461	2.0×10^{-3}	–		310,360	2.9
	Ethanol	340,372	454	1.0×10^{-3}	2.6×10^{-2}	1.1		
	Ethanol:HCl	–	450		3.3×10^{-2}	1.1		

[a] Data in dioxane.
[b] No conclusive emission could be attributed to γ-pyrone.

the n,π^* feature is now completely buried underneath the intense π,π^* band. So, in α-pyrone the two lowest lying singlet excited states, $S_1(n,\pi^*)$ and $S_2(\pi,\pi^*)$ are energetically closer than in γ-pyrone, the absorption bands due to transitions to these states appearing considerably overlapped even in non-polar media. As a consequence it was not possible to determine precisely the maxima of the n,π^* band for this molecule.

Since in the studied molecules the lowest energy state in the singlet series is n,π^* origin, it is expected that these systems show very weak fluorescence, in addition to relatively strong phosphorescence. For γ-pyrone, we have observed fluorescence in ethanol with maxima at ≈ 365 nm. However, the nature of the observed emission is questionable since the fluorescence quantum yield (ϕ_F) was found to be very weak. Solvent impurities can be ruled out of this context, which is not the case of small impurities resulting from degradation of γ-pyrone itself. As a contribution to the understanding of the nature of the observed 365 nm emission band we have measured the fluorescence excitation spectra of γ-pyrone, which were revealed to be identical both in shape and maxima to the absorption spectra. In cyclohexane, this emission was not observed. Others have observed the same fluorescence and suggested that it could be due to a protonated species of γ-pyrone [18]. The present results favor a different explanation: the close proximity of the energies of the S_1 and S_2 states in ethanol (that shall be compared with the much larger energy difference in cyclohexane, as described above) makes possible the lending of π,π^* character to S_1, thus inducing a small degree of allowance to the transition [17].

As already mentioned, in α-pyrone S_1 and S_2 are considerably closer in energy than in γ-pyrone. Hence, the observed fluorescence for this compound (see Table 2 and Fig. 2) may be due to a phenomenon analogous to that described above that justifies the observation of fluorescent emission of γ-pyrone in ethanol.

For 4HMP and 4MMP the state order for the two lowest excited singlet states was found to be the same as in the non-substituted pyrones (see Tables 1 and 2). Note that low ϕ_F values were still obtained for these compounds, though slightly larger than for the simplest compounds (Table 2). This is so because hydroxyl (and methoxyl) substitution has a marked influence on the energy of the first two singlet excited states. Theoretically, it is expected that conjugative type substitution as –OH (or $-OCH_3$) will blue shift $S_1(n,\pi^*)$ transition and red shift the $S_2(\pi,\pi^*)$ transition [19], and this trend is in fact observed for 4HMP and 4MMP relative to α-pyrone.

4.2. Triplet state properties

Upon laser excitation at $\lambda_{exc} = 266$ nm, all studied molecules exhibit $T_1 \rightarrow T_n$ in the 250–400 nm region, just after the pulse. The lowest triplet state decays by first order kinetics and can be efficiently quenched by molecular oxygen ($k_{ox} \approx 10^9\ M^{-1}\ s^{-1}$; see Fig. 4). No solvent-dependent significant changes were observed in acetonitrile and dioxane solutions.

There are no observable differences between the $T_1 \rightarrow T_n$ maxima of α-pyrone, 4HMP and 4MMP (see Table 2), an exception perhaps to the fact that for the last molecule a 280 nm depletion band is observed. The data suggest that the intersystem crossing between S_1 and T_1 is present in these molecules and can compete with internal conversion from S_1 to the ground state. In addition they also suggest that substitution of hydroxyl and methoxy groups in the α-pyrone ring does not

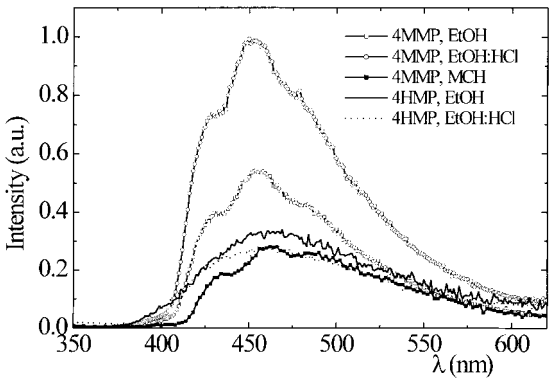

Fig. 3. Phosphorescence spectra of 4HMP and 4MMP in ethanol, ethanol/HCl (conc.) 19:1 (v/v) mixture and methylcyclohexane.

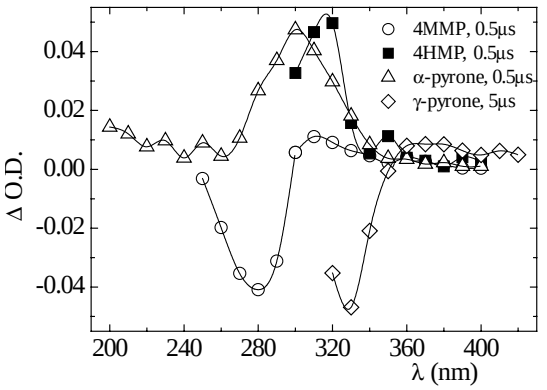

Fig. 4. Triplet–triplet spectra of (○) 4MMP, (■) 4HMP and (△) α-pyrone collected 0.5 μs after the flash, and (◇) γ-pyrone collected 5 μs after the flash.

affect greatly the absorption properties of the triplet transients (see Fig. 4).

All pyrones studied phosphoresce in rigid media at 77 K. The phosphorescence quantum yields (ϕ_P) are, for all compounds, relatively low; however, they are 1–2 orders of magnitude larger than the corresponding ϕ_F values. This indicates that the internal conversion channel is ruling out the deactivation processes from S_1 and T_1.

For α- and γ-pyrone, a single phosphorescence band was observed, independently of the solvent used, indicating that for these two compounds a neutral triplet state is formed in all cases. The same is valid for 4MMP, where the identical values for τ_{Ph}, ϕ_P, shape and maxima of phosphorescence, in the studied solvents (Table 2, and Fig. 3), support the attribution to a single, unique species, with neutral character ($N^*_{T_1}$), for the emission from T_1. For 4HMP, based on the same photophysical data, in particular on ϕ_P data and phosphorescence maxima, we believe that in acidified ethanol a cationic species ($C^*_{T_1}$) is present, whereas in ethanol this has a neutral character. Based on data relative to α-pyrone (Table 2) where a single species ($N^*_{T_1}$) seems to be present (identical ϕ_P values), we can tentatively suggest that protonation occurs on the hydroxyl rather than the carbonyl oxygen. Other explanations, such as quenching effects by chloride, are not tenable, since with 4MMP identical results are obtained in ethanol and ethanol/HCl (Table 2).

For γ-pyrone it was suggested previously that T_1 is π,π^* in nature [18]. Based on the phosphorescence lifetimes now obtained (see Table 2), it is possible now to extend this conclusion to all other studied pyrones.

4.3. Ground state properties

A complete assignment of the vibrational spectra of the different compounds in condensed phases as well as isolated in solid argon matrices was undertaken and details will be provided in a further publication. Together with the calculated geometries for the ground electronic state, vibrational spectroscopy data reveal some important details of the different intramolecular interactions operating in the studied molecules. From the results presented in Table 3 the following main conclusions can be drawn:

(i) The C_2–O bond in the α-pyrone moiety is much longer than the C_6–O bond and the two equivalent C–O bonds in γ-pyrone. In fact, the C_2–O bond length is predicted to be even longer than the C–O(H) bond length in 4HMP. These results clearly indicate that in the α-pyrones, a considerably strong repulsive interaction between the lone electron pairs of the carbonyl oxygen and O_1 exists. In addition, they also indicate that there is no significant π-electron delocalization from O_1 to the carbonyl group. In consonance with these facts, the C=O bond is shorter in the studied α-pyrones than in γ-pyrone.

(ii) The observed C–O and C=O stretching frequencies reinforce the conclusions taken in (i): νC=O appears blue shifted by ca. 60–70 cm^{-1} in the α-pyrones when compared with γ-pyrone, while within the α-pyrone moiety νC_2–O has a much lower frequency than νC_6–O (see Table 3). Very unfortunately, no comparison can be made between the νC–O frequencies observed for the α-pyrones and those of γ-pyrone, since in the first molecules the νC–O modes were found to be strongly coupled with δC–H bending vibrations (thus

Table 3
Ab initio 6-31G* calculated selected bond lengths and bond stretching frequencies and observed IR frequencies for γ-pyrone, α-pyrone and 4HMP (Bond lengths in pm; frequencies in cm^{-1}; for γ-pyrone, the frequencies given correspond to the A1 symmetric modes which were found to have a smaller coupling with other coordinates than the corresponding B1 asymmetric modes; when more than one experimental band are ascribed to a given vibration, the experimental value given in the table corresponds to the average frequency of the observed bands)

γ-pyrone				α-pyrone				4HMP			
Bond length		Stretching frequency		Bond length		Stretching frequency		Bond length		Stretching frequency	
		ν_{calc}	ν_{IR}			ν_{calc}	ν_{IR}			ν_{calc}	ν_{IR}
C=O	120.0	1757	1668	C=O	118.4	1805	1732	C=O	118.4	1797	1738
C=C	132.7	1656	1639	C_5=C_6	132.7	1659	1624	C_5=C_6	132.4	1675	1645
				C_3=C_4	133.5	1565	1543	C_3=C_4	134.4	1581	1534
C–O	134.2	907	923	C_6–O	133.9	1242	1246	C_6–O	133.2	1349	1348
				C_2–O	136.3	1110	1122	C_2–O	138.0	844	879
								C–O(H)	133.4	1246	1306
C–C	147.0	769	790	C_2–C_3	146.1	777	785	C_2–C_3	144.2	1121	1150
				C_4–C_5	144.7	949	957	C_4–C_5	144.4	940	988
								C–C(H_3)	149.4	987	991

being generally shifted to higher frequencies), whilst in γ-pyrone these modes are almost pure vibrations.

(iii) The C–C bond lengths in all compounds studied (144–147 pm) are similar to that of the central bond in butanediene (146.3 pm [20]), being significantly longer than the C–C bonds of a typical aromatic six-membered ring (ca. 139 pm). On the other hand, the C=C bond lengths (132–134 pm) do not differ very much from the C=C bond length in ethylene (133.7 pm [21]). So, the structural results indicate that no extended conjugation involving the C–C bonds occurs in the studied compounds. However, the C_2–C_3 and C_5=C_6 bonds in α-pyrone were found to have nearly the same lengths as the C–C and C=C bonds in γ-pyrone, while C_4–C_5 and C_3=C_4 were found to be, respectively, shorter and longer than those bonds (see Table 3), indicating a π-system electron density migration from the C_2–C_3=C_4 fragment towards the C_4–C_5=C_6 fragment in α-pyrone. Such migration aims to partially compensate the electron deficiency in the σ-system of the C_4–C_5=C_6 fragment due to strong electron attraction by the oxygen atoms. Note that in C_3 a back donation effect involving the carbonyl oxygen electron pairs may be operating, thus increasing the σ-density in this atom (in consonance with this interpretation, the calculated Mülliken charges in α-pyrone show that C_3 is the carbon atom having the highest electron population; (see Fig. 5).

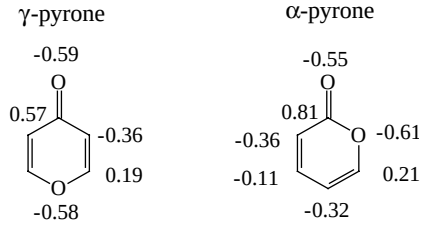

Fig. 5. Ab initio 6-31G* calculated Mülliken atomic charges for α- and γ-pyrone.

(iv) The observed C–C and C=C stretching frequencies fully support the interpretations above. In particular, a good correlation exists between the frequencies and the bond lengths (see Table 3).

(v) Finally, taking also into consideration the results of the Mülliken population analysis shown in Fig. 5, it can be concluded that, besides canonical forms I and II in Fig. 6 (the last representing essentially the polarization of the carbonyl

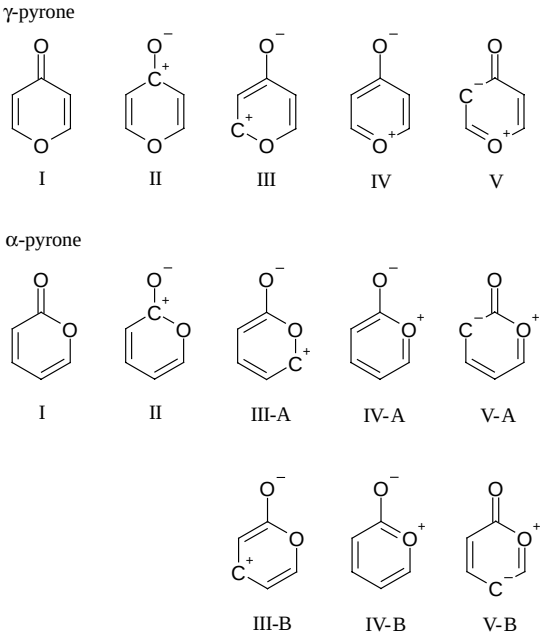

Fig. 6. Canonical forms for the α- and γ-pyrone moieties.

bond), which are clearly the dominant structures in both α- and γ-pyrone moieties, in γ-pyrone the third most important structure is with all probability canonical form III, while in the studied α-pyrones canonical forms III-A, IV-A and V-A appear to be more important than III-B, IV-B and V-B.

5. Conclusions

In all molecules studied it was found that the lowest lying singlet excited state has n,π^* character, independent of the solvent used. In contrast, triplet states of π,π^* origin were found for all pyrones. The structural and vibrational spectroscopy data for the electronic ground state demonstrated that no extensive π-system electron delocalization occurs in the pyrone moieties and enabled us to characterize the most important intramolecular interactions operating in these systems. Oxygen lone-electron pair repulsions were found to be in the origin of the longer (and weaker) C_2–O bond in α-pyrone, a result that is certainly relevant to help in understanding the chemical reactivity in this type of molecule.

Acknowledgements

The authors acknowledge financial support from "Fundação para a Ciência e Tecnologia", Lisbon (research projects PRAXIS/QUI/10137/98 and PRAXIS/PCEX/C/QUI/108/96).

References

[1] R.S. Becker, S. Chakravorti, C. Gartner, M.G. Miguel, J. Chem. Soc., Faraday Trans. 89 (1993) 1007.
[2] A. Lopes, J. Seixas de Melo, A.J. Martins, A.L. Maçanita, F.S. Pina, H. Wamhoff, E.C. Melo, Environ. Sci. Technol. 29 (1995) 562.
[3] G. Matolcsy, M. Nádasy, V. Andriska, Pesticide Chemistry, Studies in Environmental Science, vol. 32, Elsevier Science, Budapest, 1988.
[4] R.S. Becker, J. Seixas de Melo, A.L. Maçanita, F. Elisei, J. Phys. Chem. 100 (1996) 18,683.
[5] J. Seixas de Melo, R.S. Becker, F. Elisei, A.L. Maçanita, J. Chem. Phys. 107 (1997) 6062.
[6] N. Turro, Modern Molecular Photochemistry, University Science Books, Sausalito, CA, 1991.
[7] W.J. Hehre, R. Ditchefield, J.A. Pople, J. Chem. Phys. 56 (1972) 2257.
[8] M.J. Frisch, G.W. Trucks, H.B. Schlegel, P.M.W. Gill, B.G. Johson, M.A. Robb, J.R. Cheeseman, T. Keith, G.A. Petersen, J.A. Montgomery, K. Raghavachari, M.A. Al-Laham, V.G. Zakrzewski, J.V. Ortiz, J.B. Foresman, J. Cioslowski, B.B. Stefanov, A. Nanayakkara, M. Challacombe, C.Y. Peng, P.Y. Ayala, W. Chen, M.W. Wong, J.L. Andres, E.S. Replogle, R. Gomperts, R.L. Martin, D.J. Fox, J.S. Binkley, D.J. Defrees, J. Baker, J.P. Stewart, M. Head-Gordon, C. Gonzalez, J.A. Pople, GAUSSIAN 94 (Revision E.2), Gaussian Inc., Pittsburgh PA, 1994.
[9] R. Fausto, TRANSFORMER (version 2.0), Departamento de Química, Universidade de Coimbra, Portugal, 1996.
[10] M.D.G. Faria, R. Fausto, BUILD-G and VIBRAT (version 2.0), Departamento de Química, Universidade de Coimbra, Portugal, 1996.
[11] M.J.S. Dewar, R.C. Bingham, D.H. Lo, J. Am. Chem. Soc. 97 (1975) 1285.
[12] M.C. Zerner, in: K.B. Lipkowitz, D.B. Boyd (Eds.), Semiempirical Molecular Orbital Methods, Reviews in Computational ChemistryVCH, New York, 1991, pp. 313–365.
[13] J.E. Ridley, M.C. Zerner, Theor. Chim. Acta 32 (1973) 111.
[14] J.J.P. Stewart, MOPAC 6.0, USA, 1990.
[15] HYPERCHEM 3.0, Hypercube Inc., Canada.

[16] M.A. Thompson, ARGUS™, v. 1.2, USA, 1996.
[17] J. Seixas de Melo, R.S. Becker, A.L. Maçanita, J. Phys. Chem. 98 (1994) 6054.
[18] N. Ishibe, H. Sugimoto, J.B. Gallivan, J. Chem. Soc., Faraday Trans. 2 71 (1975) 1812.
[19] R.S. Becker, Theory and Interpretation of Fluorescence and Phosphorescence, Wiley/Interscience, New York, 1969.
[20] J.E. Rice, B. Liu, T. Lee, C.M. Rohlfing, Chem.Phys. Lett. 161 (1989) 277.
[21] D.R. Lide, Tetrahedron 17 (1962) 125.